FELIX Potential for small-x Parton Measurements in proton-proton (-nucleus) Collisions

Lyndon Alvero, Mark Strikman and Jim Whitmore
Physics Department, Pennsylvania State University
104 Davey Lab., University Park, PA 16802-6300, U.S.A.

30 January 1997

Abstract

We present calculations of several pp scattering cross sections which can be studied at the LHC. Significantly large rates for momentum fraction, x, as low as 10^{-6} are obtained, allowing for possible extraction of quark and gluon densities in the proton and nuclei down to these small x values.

1 Introduction

Upon completion of the Large Hadron Collider (LHC) at CERN and with the availability of a full acceptance detector like FELIX, a whole new era of high energy physics measurements and studies will begin. Operating at luminosities of order 10^{31} cm^{-2}s^{-1} and center of mass energy of about 14 TeV, FELIX will provide a testbed of new physics phenomena, and has the potential to generate events corresponding to regions of phase space that are currently inaccessible experimentally.

One important application that may be studied at the LHC is the measurement of quark and gluon distribution functions inside the proton at very small momentum fractions x. In this note, we consider several high energy proton-proton processes and show that even in the region $x \sim 10^{-6}$, a significant number of events can still be observed. By imposing the right cuts, one can show how the parton distributions may be extracted. All the calculations were performed in lowest order perturbative QCD. We also used CTEQ3 [1] for the proton parton distributions.

Although our results were obtained from pp interactions, the same analysis can be easily applied to pA or proton-nuclei studies as well. For example, in the case of p Ca (calcium nucleus) scattering at center of mass energy 63 TeV, the region $x \sim 10^{-6}$ can also be probed. Data from this type of study can also provide information on parton distributions inside nuclei for both small and large values of x.

For luminosities of 10^{31} cm^{-2}s^{-1} and using 10^7 sec/year, one can obtain integrated luminosities of about 100 pb^{-1}/year. In the case of pA collisions, the loss in the integrated luminosity is to a large extent compensated for by cross sections which are approximately proportional to the atomic number of nucleus A.

2 Kinematics and cross sections

We consider the following hadronic processes

$$\begin{aligned} p(p_1)+p(p_2) &\rightarrow \mathrm{jet}_1+\mathrm{jet}_2+X \quad (\mathrm{JJ}), \\ p(p_1)+p(p_2) &\rightarrow \mathrm{jet}+\gamma+X \quad (\mathrm{J}\gamma), \\ p(p_1)+p(p_2) &\rightarrow \mathrm{Q}+\bar{\mathrm{Q}}+X \quad (\mathrm{Q}\bar{\mathrm{Q}}), \end{aligned} \tag{1}$$

where Q($\bar{\mathrm{Q}}$) denotes a heavy quark (antiquark), at center of mass energy $\sqrt{s} = 14$ TeV with $s = (p_1 + p_2)^2$.

The cross section for process A in eq. (1) is given by

$$\sigma^A = \sum_{a,b} \int dx_a \int dx_b \int dp_T \frac{2p_T}{[1 - \frac{4p_T^2}{x_a x_b s} - \frac{4m_Q^2}{x_a x_b s}\delta_{I,Q\bar{Q}}]^{1/2}} f_{a/p}(x_a, \mu) f_{b/p}(x_b, \mu) \frac{d\sigma_{ab}^A}{d\hat{t}}, \tag{2}$$

where $f_{a/p}(x_a, \mu)$ is the number density of parton a, with momentum fraction x_a, in the proton, p_T is the transverse momentum of the outgoing jet or heavy quark, m_Q is the heavy quark mass and $\frac{d\sigma_{ab}^A}{d\hat{t}}$ denotes the partonic hard scattering coefficient. For the two jet cross section, the sum in eq. (2) runs over the gluon and all quark, antiquark flavors. The lowest order form of $\frac{d\sigma_{ab}^{JJ}}{d\hat{t}}$ may be found in [2]. For the two other cases, jet plus photon and heavy quarks in the final state, only two partonic processes contribute in leading order, $Gq \to q\gamma, q\bar{q} \to G\gamma$ and $GG \to Q\bar{Q}, q\bar{q} \to Q\bar{Q}$, respectively. The relevant partonic coefficients may be found in [3].

We chose $p_{T,min} = 10$ GeV in our calculations. Note that for asymmetric x_1, x_2 configurations, in which we are mostly interested, both jets are produced at very large rapidities, y. For such y, soft interactions result in much smaller underlying event E_T pedestals than for $y \sim 0$. This holds for pA collisions as well. Hence, our choice of $p_{T,min}$ appears safe enough. Kinematics also require that the inequality

$$x_1 \geq \frac{4p_{T,min}^2}{x_2 s} \tag{3}$$

be satisfied. Using $\sqrt{s} = 14$ TeV, one then determines that the momentum fractions x_i obey $x_1 x_2 \geq 2.041 \times 10^{-6}$.

3 Jet plus photon

Using eq. (2), we calculate the cross section for producing a jet and a photon in bins of p_T and x_1, and with the parameter x_2 integrated up to 0.8. The color plot of the resulting (p_T, x_1) distribution is shown in Fig. 1, where the color coded bar at the right gives the cross section in pb. One readily observes that large cross sections are obtained, as large as $\sim 10^5$ pb, in the entire range of x_1 with 10 GeV $\leq p_T \leq$ 50 GeV. Combined with the integrated luminosity quoted earlier, this translates into a significant number of jet + photon events per year.

The cross section (solid curve) in bins of x_1 is shown in Fig. 2, where the contributions coming from the Gq (dashed curve) and $q\bar{q}$ (dot-dashed curve) channels are also shown. The cross section is dominated by the Gq channel which is at least 10 times larger than the contribution of the $q\bar{q}$ channel in the entire x_1 range. Using large x quark distributions extracted in other experiments, one may then extract the gluon density for very small x in the range $x \geq 2.6 \times 10^{-6}$ from this type of cross section.

4 Heavy Quarks

We next consider the cross section for the production of charm quarks. Fig. 3 shows a color plot of the cross section in bins of p_T and x_1, with x_2 integrated up to 0.8. Again, large values are obtained in the entire x_1 range, with the bulk coming from the region 10 GeV $\leq p_T \leq$ 50 GeV where the cross section is of order 10^6 pb.

In Fig. 4, we show the x_1 distribution of the cross section. Aside from the total cross section (solid curve), we also exhibit the contributions from the two active partonic channels, GG (dashed curve) and $q\bar{q}$ (dot-dashed curve). One finds that the cross sections are of order 10^6 pb when $10^{-5} \leq x_1 \leq 10^{-1}$. In the region $2.6 \times 10^{-6} \leq x_1 \leq 10^{-5}$, the cross section drops to about 2.7×10^4 pb. However, at LHC luminosities, this still translates to a significant number of events per year, of order 10^6. Most of the cross section comes from the GG

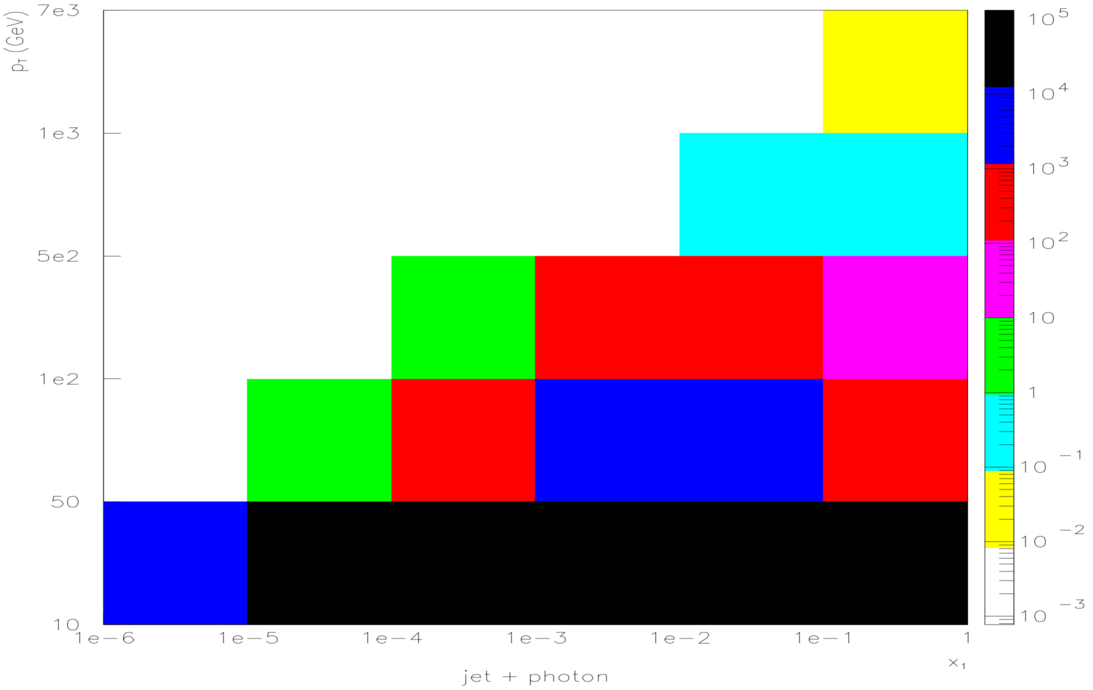

Figure 1: The (p_T, x_1) distribution for Jet + γ production. The color coded bar at the right gives the cross section in pb.

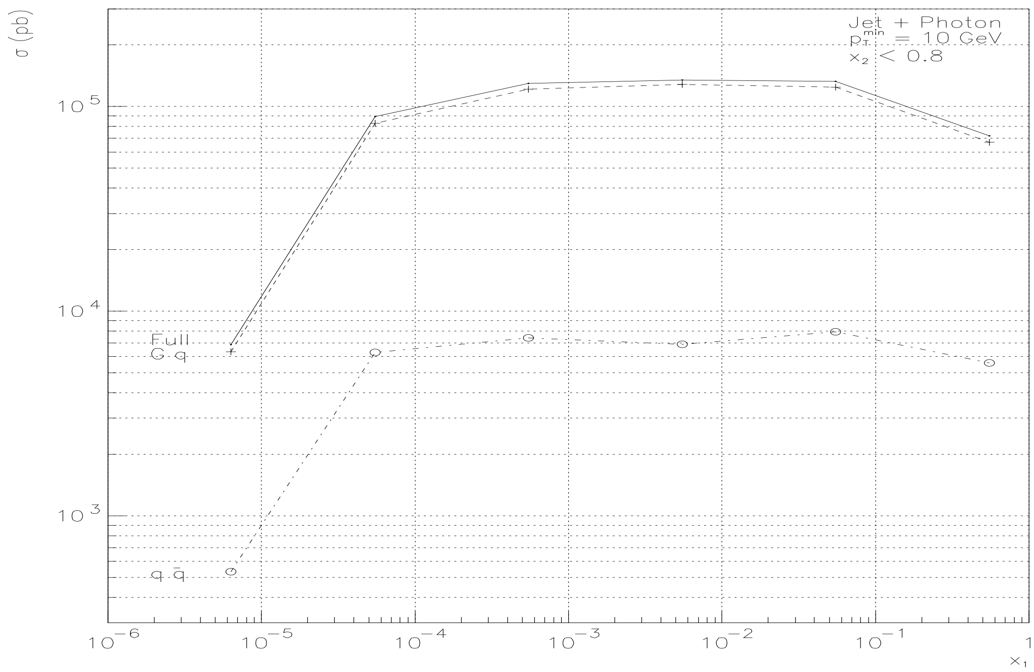

Figure 2: The x_1 distribution for Jet + γ production.

channel which is about 10 times larger than the $q\bar{q}$ contribution for $x_1 > 10^{-5}$. In the region $x_1 < 10^{-5}$, the GG cross section is still larger but the ratio falls to about 1.35.

Imposing a stricter cut in x_2, $0.6 \leq x_2 \leq 0.8$, one obtains the cross sections in Fig. 5. The cross section now falls very steeply with x_1. In the first bin ($x_1 \leq 10^{-5}$), the total cross section is about 10^3 pb or about 10^5 events per year at the LHC. More importantly, in this region of x_1, the $q\bar{q}$ contribution now becomes twice that of GG. Using the gluon density obtained from the jet plus photon cross section as described in the previous section, the background consisting of GG channel contributions is well determined. This is then an excellent region for extracting the quark density.

5 Two Jets

We show in Figs. 6 and 7 the (p_T, x_1) and x_1 distributions for dijet production, respectively, with x_2 integrated up to 0.8. The same general features as in the plots for heavy quark and jet plus photon are observed. However, one also notes that the dijet cross section is about 100 times bigger than either of the previous two cross sections. This is expected because now all partonic channels contribute, and as can be seen from Fig. 7 the cross section is dominated by the GG and Gq channels.

This interaction process now provides an independent consistency check of the parton distributions obtained from the other processes described in previous sections.

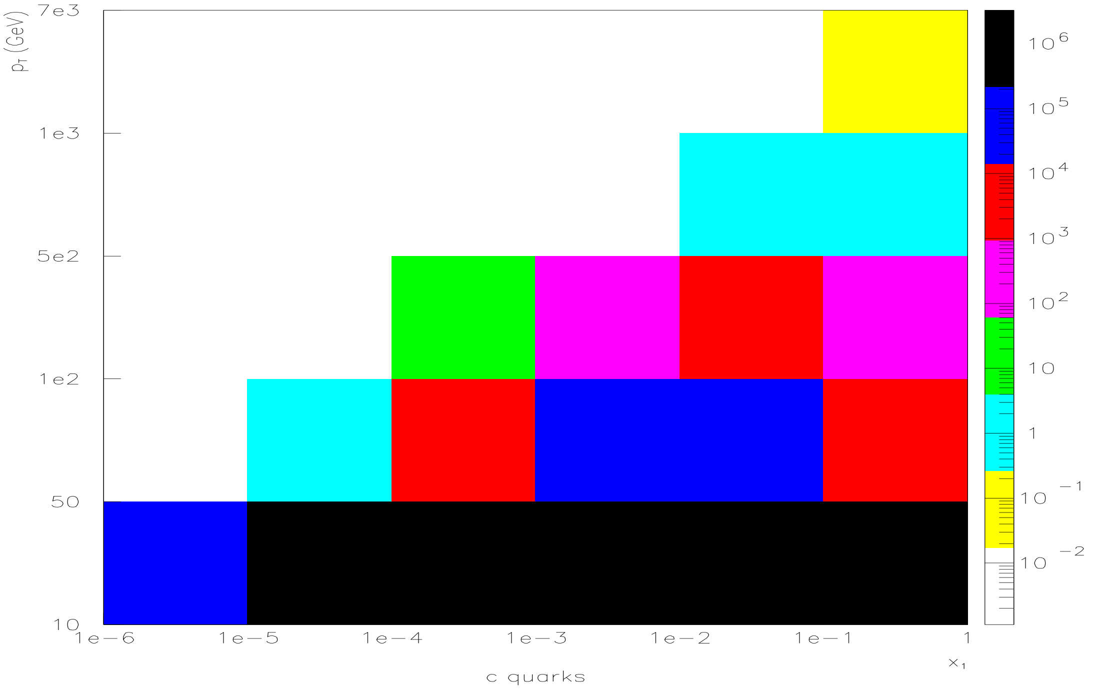

Figure 3: The (p_T, x_1) distribution for charm quark production. The color coded bar at the right gives the cross section in pb.

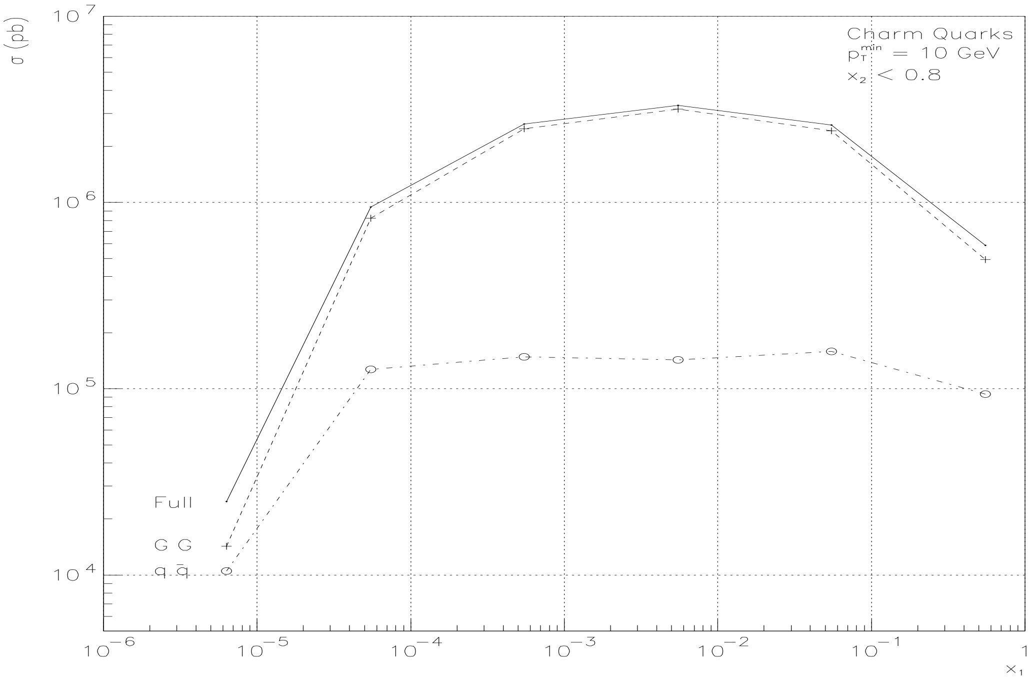

Figure 4: The x_1 distribution for charm quark production.

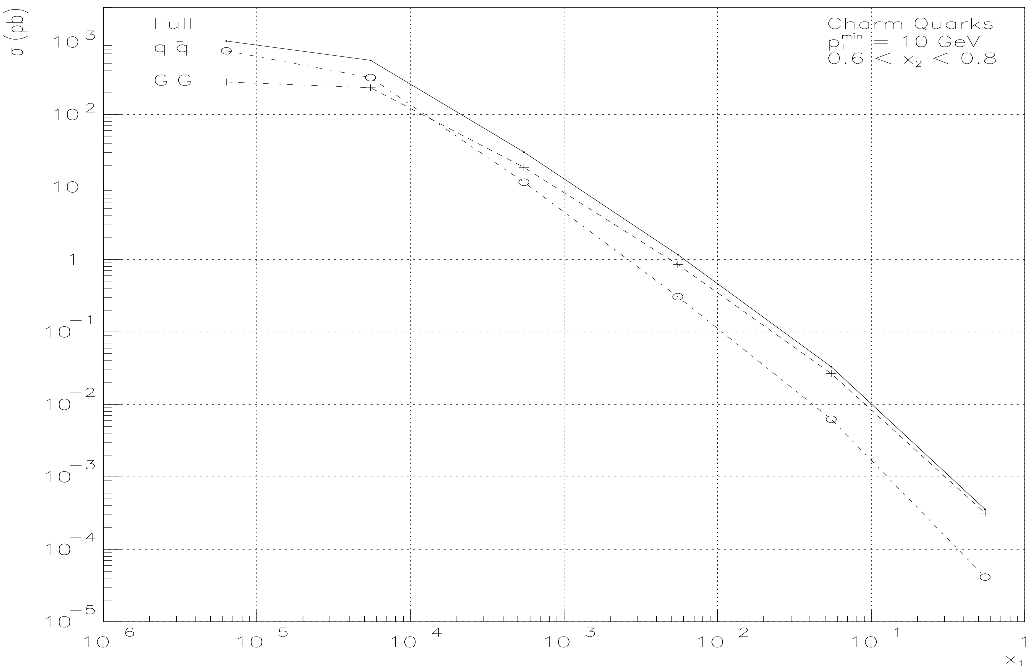

Figure 5: The x_1 distribution for charm quark production with a stricter cut in x_2.

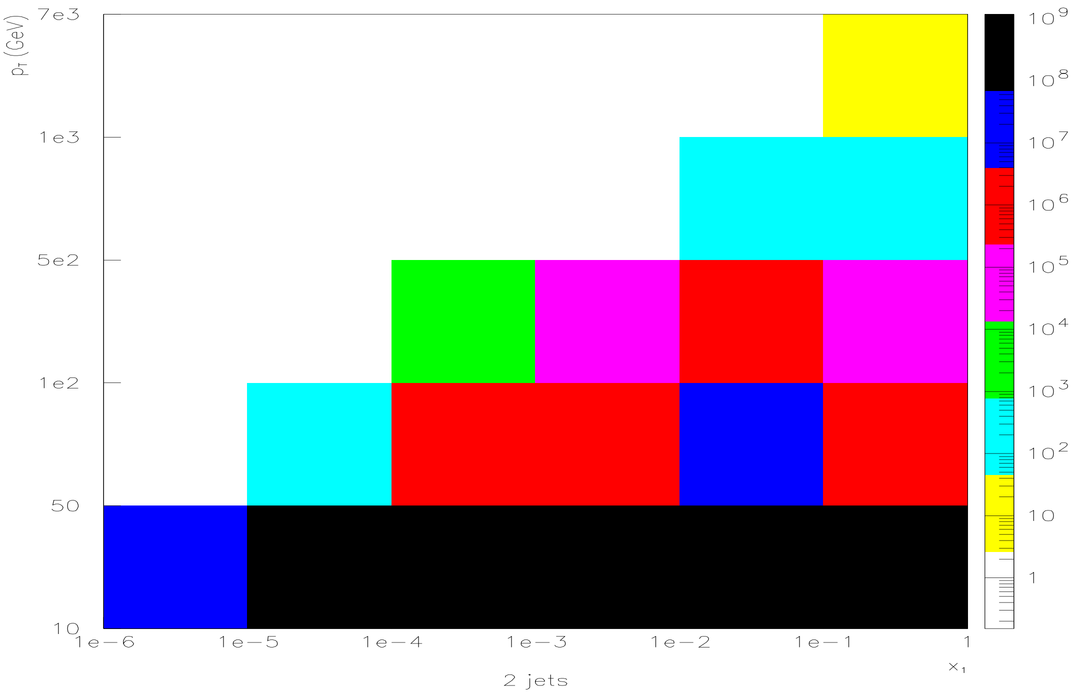

Figure 6: The (p_T, x_1) distribution for dijet production. The color coded bar at the right gives the cross section in pb.

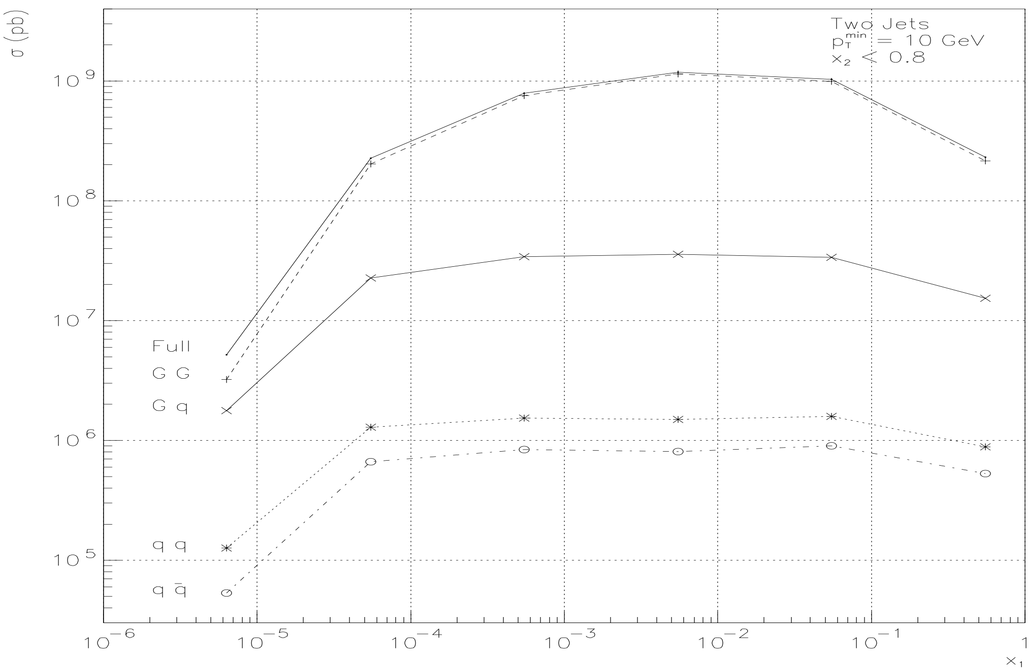

Figure 7: The x_1 distribution for dijet production.

6 Conclusions

To summarize, we find that due to its unique forward acceptance, FELIX offers the opportunity to measure parton distributions in nucleons and nuclei (nuclear shadowing) down to $x \sim 10^{-6}$ in several independent ways which provide a number of cross checks for the pQCD interpretation of the measurements.

References

[1] The CTEQ parton distributions can be obtained from `http://www.phys.psu.edu/~cteq/`.

[2] E. Eichten, I. Hinchliffe, K. Lane and C. Quigg, Rev. Mod. Phys. 56 (1984) 579; 58 (1986) 1065.

[3] CTEQ Collaboration, "Handbook of Perturbative QCD Version 1.0", April 1993.